Transient thermo-hygrometric CFD model of Trombe wall system

Nour El Zein, Yacine Ait Oumeziane, Philippe Desevaux, Sylvie Bégot, Valérie Lepiller

FEMTO-ST Institute, Université de Franche-Comté, CNRS, Belfort, France

nour.elzein@femto-st.fr ,yacine.aitoumeziane@femto-st.fr, philippe.desevaux@univ-fcomte.fr, sylvie.begot@univ-fcomte.fr, valerie.lepiller@univ-fcomte.fr

Abstract

The objective of this study is to develop a transient CFD model representing the dynamic behavior of Trombe walls. The current model takes into consideration variable solar radiation as well as the presence of occupants and their activities. The temperature and velocity profiles at different locations are plotted. The moisture's impact on the hygrothermal behavior is then investigated. The results show that the relative humidity distribution inside the system is mainly influenced by the ventilation strategy in which the moisture is accelerated and transported by the flow in the case of vents opening. The finding revealed that the maximum relative humidity (RH) reached in the system doesn't exceed 22%. However, due to the lower temperature values observed in the system during overcast winter nights, there is a potential condensation risk on glass and wall surfaces. Furthermore, the results indicate that the Trombe wall can ensure the occupant's thermal comfort from 11 am to 4 pm during overcast wintertime.

Nomenclature

AAC aerated cellular concrete

C_p specific heat, J.kg⁻¹. K⁻¹

D_m moisture diffusivity, m².s⁻¹

D_T thermal diffusivity, m².s⁻¹

DO Discrete ordinate

hext heat transfer coefficient, W.m⁻².K⁻¹

Ji moisture diffusion, kg.s⁻¹.m⁻²

Ri Reaction

RH relative humidity, %

S_i source term

Sct Schmidt number

T temperature, K

t time, s

UDF user-defined function

v velocity m.s⁻¹

Wv water vapor

Y_i local mass fraction of each species

CFD Computational Fluid Dynamics

Greek symbols

α absorptivity

ε emissivity

λ conductivity, W.m⁻¹. K⁻¹

μ Dynamic viscosity, kg.m⁻¹. s⁻¹

ρ density, kg.m⁻³

τ transmissivity

Index and exponent

a air

i species

r radiation

t turbulent

1. Introduction

In the context of the current worldwide energy situation, the building sector stands as a substantial contributor to worldwide energy consumption and the emission of greenhouse gases. Therefore, to improve the building's energy performance and hygrothermal comfort, it is crucial to adopt renewable energy resources and eco-friendly engineering solutions. Among various technologies, Trombe walls, are recognized as a cost-effective solution to reduce

energy consumption. Nevertheless, the traditional Trombe wall design presents numerous benefits, it also has drawbacks such as overheating, heat loss, and reverse thermo circulation which require a careful selection of its design parameters and operation management.

Several theoretical and experimental studies have been carried out to investigate the thermal behavior of Trombe walls under various weather conditions and evaluate the impact of its geometrical parameters on its overall thermal efficiency. However, to date, very few developed CFD models take into account the dynamic behavior of such a system, and most of the available models in the literature do not consider the effect of moisture on Trombe walls as the focus is often on the determination of its thermal efficiency.

Despite the importance of insulation in decreasing heat loss, numerous researchers have pointed out that introducing insulation layers into Trombe walls could lead to potential moisture accumulation or condensation on the wall surface, especially in extreme climatic conditions [1],[2]. Therefore, it is important to maintain normal moisture conditions for ensuring occupant comfort, and reliable operation of facade systems. Few numerical analyses have examined the impact of moisture on Trombe walls during the overcast winter season. The occurrence of these moisture-related issues is determined by the system's specific temperature difference and relative humidity levels. In addition, in the literature, only a few numerical studies have been identified that analyze the effect of relative humidity on Trombe walls in hot humid weather conditions. In such climatic conditions, the amount of moisture content in the air is dissimilar and may vary by 10g of moisture per kg of dry air compared to dry climate which highly affects the performance of solar chimneys as stated by Sudprasert et al.[3]. Through a 2D steady-state CFD model and by considering uniform temperature, the authors have compared the effect of moist air on the temperature and velocity profiles of the solar chimney in Thailand. The results indicate a reduction of the average velocity in the gap and a higher air temperature at the outlet when increasing the relative humidity. On the other hand, Dahire et al. [4] have developed a numerical model of solar roof chimneys and analysed the effect of relative humidity on the performance of the chimney channel by considering the moist air as a participating medium to radiation. Their results support the other studies. The authors underline that increasing relative humidity at constant temperature leads to a decrease in the air mixture density which in turn results in a decrease of the air mass flow rate due to a reduction in buoyancy. However, it is well recognized that steady-state models do not properly represent system behavior because unstable climatic factors result in unstable surface temperature distribution. This is also impacted by the thermophysical properties and the geometrical design parameters such as the thickness and the height of the wall. Indeed, research done by El-Sherief et al. [5] has demonstrated that in the case of high solar radiation, a humidifier placed at the back of the solar chimney can increase the velocity of the solar chimney and enhance the natural convection process. Consequently, there is a need for a more accurate model capable of capturing the dynamic behavior of such a system to analyze how design decisions affect the performance of Trombe walls and hygrothermal comfort.

This paper aims to develop a transient CFD model that simulates the dynamic behavior of a conventional Trombe wall. Since there is no a priori method for establishing optimal numerical parameters, mesh grid, and time step sensitivity analysis are first performed. Then, several user-defined functions and sources are implemented to take into consideration variable solar radiation as well as the presence of occupants and their activities.

2. Model description

2.1 Model geometry

The CFD model is based on the geometric specifications of an existing Trombe wall test bench located at the laboratory, which has dimensions of 2x1.97 meters in width and height respectively. The experimental model represents a typical Trombe wall coupled to a room. The glass is 8mm thick, and the thermal storage wall is made of 20 cm thick aerated cellular concrete. The room walls are insulated on the outside with a layer of thick polystyrene to reduce heat loss. A solar simulator consisting of 18 halogen lamps is used to replicate the solar radiation ranging from 0 to $1000W.m^{-2}$. Our case study covers the same boundary conditions and material properties of the experimental test bench. The room walls are assumed to be adiabatic. At the glass surface, a combination of convection and radiation conditions is taken into account. The heat transfer coefficient is determined using the following correlation: $h_{ext} = 5.7 + 3.8v_{wind}$ [6].



25cm 19.5cm 19.5cm 25cm 19cm20cm

Figure 1: View of the test bench

Figure 2: Test bench dimensions

| Thermophysical properties | ρ (kg.m ⁻³) | C_p (J.kg ⁻¹ . K ⁻¹) | λ (W.m ⁻¹ . K ⁻¹) | ε | α | τ |
|---------------------------|-----------------------------------|---|---|------|------|-----|
| Glass | 2500 | 800 | 1.020 | 0.89 | - | 0.9 |
| Polystyrene | 30 | 1450 | 0.038 | 0.90 | 0.1 | |
| Aerated concrete | 450 | 1000 | 0.110 | 0.85 | 0.95 | |

Table 1: Thermal properties of the physical model

2.2 Sensitivity analysis

To calibrate the model, a preliminary analysis is conducted to assess the sensitivity of the results to grid and timestep size. Fixed boundary conditions, as represented in Figure 3, are selected to conduct this analysis. To investigate heat transfer and fluid dynamics, governing equations that address energy, momentum, and mass conservation are used. Specifically, we incorporate the DO (Discrete Ordinate) radiation model and k-ω SST technique, along with the Boussinesq approach, to effectively address turbulence and natural convection phenomena. The average wall temperature is used as a reference point, and the relative error is employed as a metric to evaluate the results' dependency on mesh size. The results as represented in Figure 4, indicate that, among all the cases considered, meshes of size 3mm and 5mm exhibit convergences, with relative errors less than 1% affirming these mesh's capability to accurately capture the temperature distribution in this region. For the timestep size analysis (Figure 5), a

more sophisticated approach is adopted to compare results, involving the utilization of a regression algorithm for extrapolating all data points. Subsequently, Mean Absolute Error (MAE) and Root Mean Square Error (RMSE) are employed as metrics to assess the performance of the predictive model. Following the validation of the predictive model, relative error is used to determine the appropriate timestep size. Consequently, a mesh size of 5mm and timesteps of 10s are selected for further analysis.

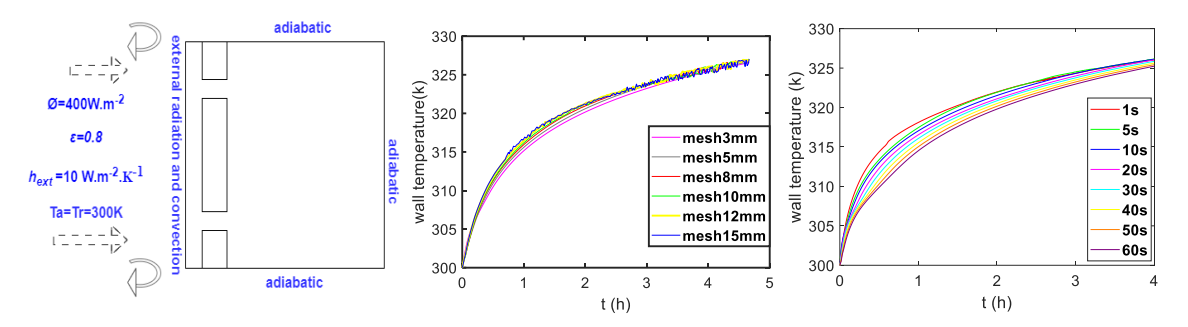


Figure 3: Boundary conditions

Figure 4: Mesh size effect

Figure 5: Time step effect

2.3 Description of the species model in Ansys fluent

The moisture transport in the air involves convection and diffusion mechanisms, as represented in Equation (1)

$$\frac{\partial}{\partial t} (\rho Y_i) + \nabla \cdot (\rho \vec{\nu} Y_i) = -\nabla \vec{J}_i + R_i + S_i$$
(1)

where R_i is the reaction mechanism and S_i is the source term.

The diffusion of water vapor in air as represented in Equation (2) is described by Fick's law, which asserts that the diffusion process is directly proportional to the mass fraction. Additionally, this model incorporates thermal diffusion, commonly referred to as the Soret effect. The influence of turbulence on diffusion is considered by the introduction of the turbulence diffusion coefficient. This coefficient is computed as the viscosity ratio to the Schmidt number, encapsulating the impact of turbulence on the overall diffusion dynamics. [7]

$$J_i = -\left(\rho D_{i,m} + \frac{\mu t}{S_{ct}}\right) \nabla Y_i - D_{T,i} \frac{\nabla T}{T}$$
 (2)

2.4 Thermo-hygrometric model specification

In reality, solar radiation follows a complicated and dynamic pattern. Factors such as the angle of incidence, atmospheric conditions, and seasonal fluctuations in solar intensity provide significant obstacles in precisely modeling a realistic representation. The simulation of solar radiation using a sinusoidal function may serve as a simplified representation of the temporal variation of solar radiation on the Trombe wall surface throughout the day. Therefore, a dataset obtained from PVGIS[8] is simulated, specifically focusing on the weather conditions during overcast winter days in Belfort in the month of January. A UDF (User Defined Function) has been developed to replicate solar radiation. As shown in Figure 6(a), it follows a sinusoidal pattern, with the intensity of direct and diffuse solar radiation increasing gradually from 8:30 am, and reaching its peak at 12:30 pm, reaching a maximum value of 317 W.m⁻² for direct radiation and 137 W.m⁻² for diffuse fraction. Subsequently, the solar radiation gradually decreases, ultimately reaching its minimum at 5:40 pm. The outdoor temperature is fixed to 2°C.Furthermore, in order to simulate the occupant's moisture generation and by considering the moisture generation of a single-family ranged from 1 to 20kg/day [9], and the presence of occupants or their absence is a function of space and time, an UDF following the sine function

is implemented and introduced into the model as a moisture source at the location of room center as represented in Figure 6 (c). However, it is important to note that a previous experimental study [10] focusing on investigating the airflow characteristics of humans using manikin has demonstrated the occurrence of thermal plume directed vertically with a max velocity value reached equal to 0.18m.s^{-1} and by taking into account that heat generation rate by human ranged from 35 to 80W.m^{-2} depending on their activities [11], it is decided to include those effects by implementing another UDF as an energy source.

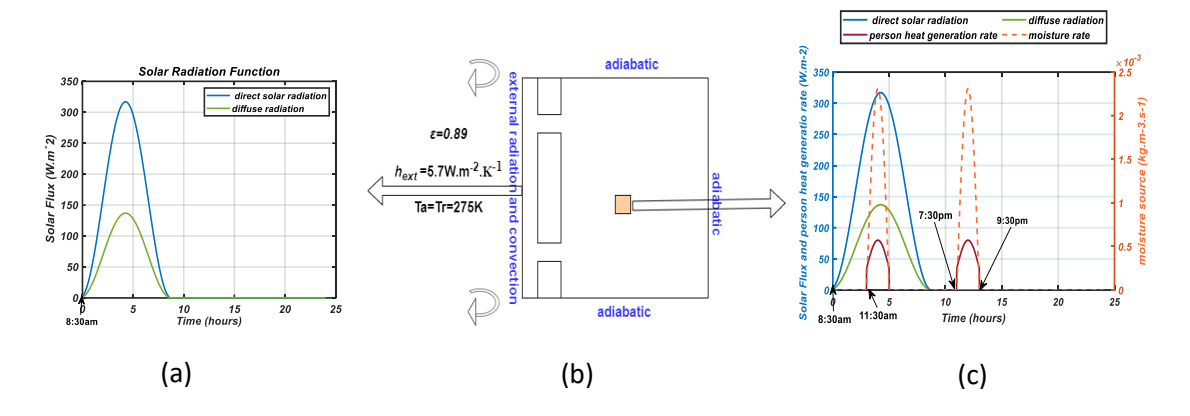


Figure 6: Humidity model boundary conditions

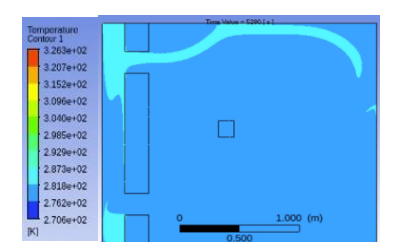
In addition to the thermal model consisting of the DO radiation model and k- ω SST turbulence model, a species model is required to model the moisture transport in air, in which the moist air is considered as a mixture of dry air and water vapor. For the mixture model, the Boussineq approach is no longer compatible with the species model [7]. Therefore, the incompressible ideal gas hypothesis is assumed to express the relation between temperature and density. Mixing law is used to express the relation of the temperature on Cp. The thermophysical properties of the mixture model are summarized in Table 2.

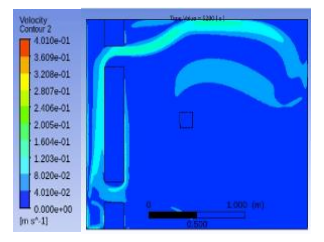
| Properties | ho | C_p | λ | μ | D_m | D_T | |
|------------|-----------------------|--|---------------------|---|-----------------------|----------------|--|
| | (kg.m ⁻³) | (J.kg ⁻¹ .K ⁻¹) | $(W.m^{-1}.K^{-1})$ | (kg.m ⁻¹ . s ⁻¹) | $(m^2.s^{-1})$ | $(m^2.s^{-1})$ | |
| Air | Ideal gas | 1600 | 0.024 | 1.789.10 ⁻⁵ | - | - | |
| Wv | Ideal gas | cp(T) | 0.0261 | 1.34.10 ⁻⁵ | - | - | |
| Mixture | ideal gas | Mixing law | Mixing law | 1.72.10 ⁻⁵ | 2.88.10 ⁻⁵ | Kinetic theory | |

Table 2: Mixture model properties

3. Results

To provide a comprehensive investigation of the behavior of Trombe walls, it is important to analyze the temperature, velocity, and H_2O mass fraction profiles at different times. Notably at 10 am (Figure 7 (a,b,c)) corresponding to the phase of solar sunshine without occupants' presence, it is shown the thermal buoyancy effect induced by the convection process causing the air density to decrease. As a result, the heated air rises and circulates to the adjacent area through the upper vent.





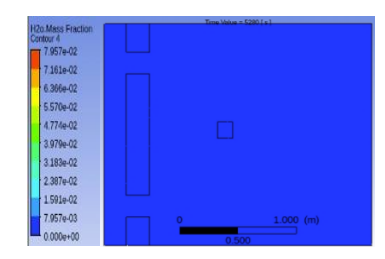
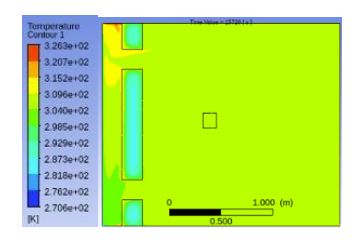


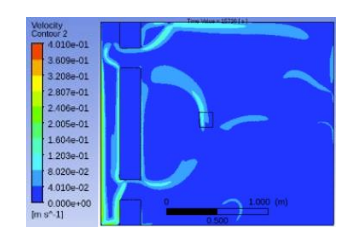
Figure 7: (a)Temperature profile

(b)Velocity profile

(c)Vapor mass fraction

At 12:30 pm (Figure 8(a, b,c)) corresponding to a scenario where occupants are present during sunshine hours, and their activities contribute to the thermal dynamics of the indoor environment, it is observed, the thermal plume formed by occupants in which the upward air speed reached 0.16 ms⁻¹. Furthermore, it is shown the moisture distribution inside the system is primarily impacted by the buoyancy effect. As warm air rises within the room, it carries moisture with it, leading to a distributed vapor mass fraction inside the room rather than on the cavity side.





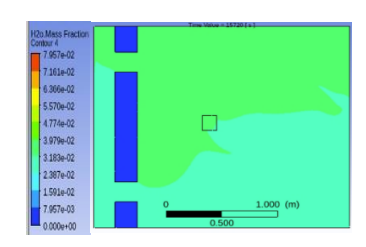
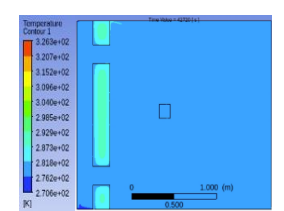
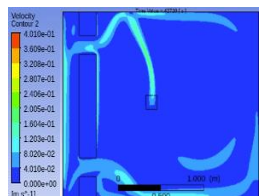


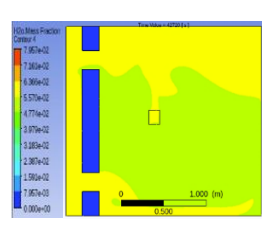
Figure 8: (a)Temperature profile (b)Velocity profile

(c) Vapor mass fraction

At 8 pm (Figure 9(a, b,c,d)) corresponding to the phase of occupant presence during the night, it is shown that the reverse flow moves the warm moist air vertically leading to the distribution of moisture from the cavity side toward the room side.







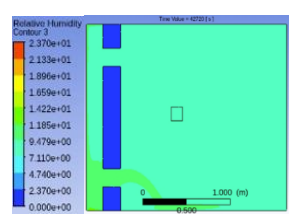


Figure 9: (a) Temperature profile(b) Velocity profile(c) Mass fraction (d)RH profile

3.1. Daily behavior of Trombe wall

In order to check the functionality of the implemented UDF as well as the convergence of the results, different monitoring points are considered at different locations of the geometry as illustrated in Figure 10.

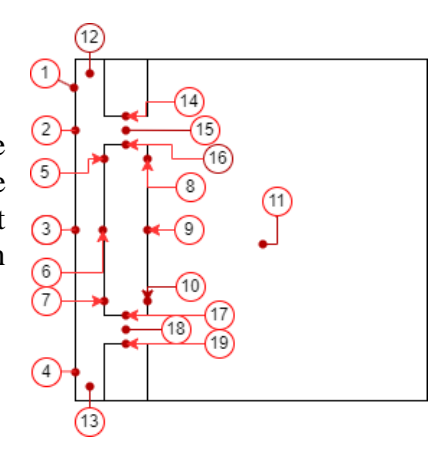
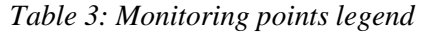


Figure 10: Monitoring points location

| Position sensors | Glass | Outside | Inside | Room | Upper | Lower | Cavity |
|------------------|---------------------------|---------------------|----------------------|--------|------------------------|------------------------|-----------------|
| | | wall surface | wall surface | center | Vent | vent | |
| Sensor's name | pt 1, pt 2, pt 3, pt 4 | pt 5, pt 6, pt 7 | pt 8, pt 9, pt 10 | pt 11 | pt 14, pt 15, pt 16 | pt 17, pt 18, pt 19 | pt 12, pt 13 |



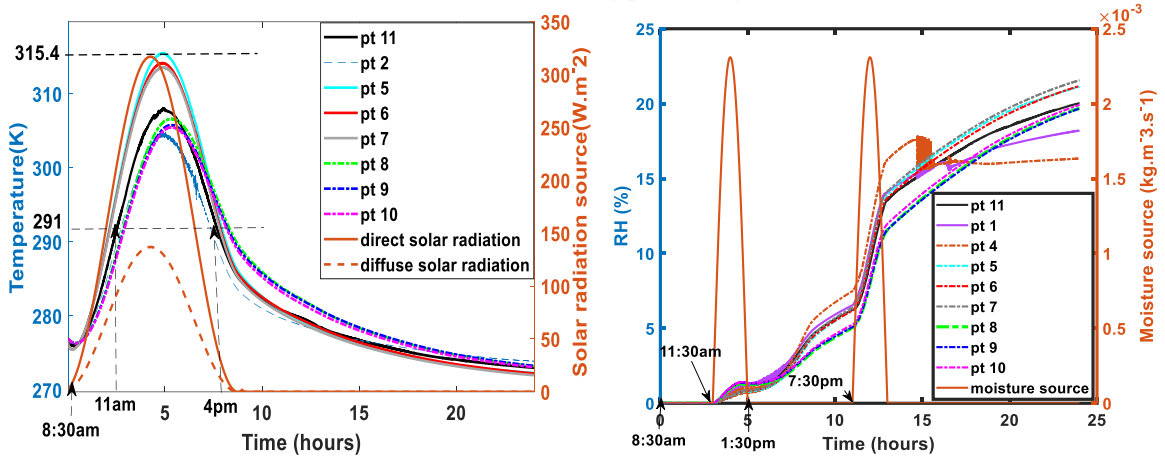


Figure 11: Temperature profile

Figure 12: Relative humidity

The temperature distribution at the monitored points is first plotted in Figure 11. It shows the behavior of a typical Trombe wall during winter daytime. Notably, as the solar radiation increases, the outside wall surface experiences heating with a time lag of 50min, reaching a maximum temperature of 315K. Analysis indicates temperature homogeneity at various sections of each wall side, with the maximum difference found to be 1.5K. It was also observed that the room temperature was influenced by solar intensity, particularly as the warm air circulated and heated the interior space during daylight hours. Furthermore, it is shown that at the time of the introduction of the moisture source, the temperature profile of the room center is affected. After the end of solar radiation, the temperature at all monitored locations decreases. However, it is observed that the inside wall surface surpasses the cavity side, indicating the thermal insulation properties of AAC. Assuming an indoor comfort temperature minimum of 291K, the findings demonstrate that the Trombe wall can provide the occupant thermal comfort from 11 am to 4 pm during overcast wintertime. This necessitates the implementation of an adequate ventilation strategy and vents operation management technique to mitigate reverse airflow and consequent heat losses.

Figure 11,12 demonstrate the correlation between temperature and RH, indicating that an increase in the air temperature during the injection of the moisture source leads to an increase of the air moisture content resulting in a slightly increase in RH levels. However, the temperature decreases at night which leads to a fast increase in RH levels. Also, it is shown the correlation between the RH levels at various monitoring points and the RH at the room center, especially due to the opening of vents. The synchronized trends across all monitoring points emphasize the influence of the vents control strategy on the distribution of relative humidity and hygrothermal behavior of the system. Furthermore, the analysis reveals that the maximum RH attained in the system is 22%. Taking into account that the temperature of the outside wall and glass surface reaches 2 °C at night, this leads to the potential occurrence of condensation risks at these regions during this period.

4. Conclusion

This article presents a numerical analysis of the transient behavior of the Trombe wall. A methodology for modeling the humidity effect on Trombe walls is proposed. To compare the results, the temperature, velocity, and relative humidity profile in function of the implemented UDF are plotted. The results demonstrate the interactions between airflow, temperature, and moisture distribution in the Trombe wall which is crucial for designing and operating buildings that provide comfortable and healthy indoor environments, particularly during night-time occupancy. The results indicate that the Trombe wall can effectively maintain the occupant thermal comfort from 11 am to 4 pm during overcast wintertime. However, the study also highlights the potential occurrence of condensation risk at night under similar weather conditions.

5. References

- [1] K. Sergei, C. Shen, and Y. Jiang, 'A review of the current work potential of a trombe wall', *Renew. Sustain. Energy Rev.*, vol. 130, p. 109947, Sep. 2020, doi: 10.1016/j.rser.2020.109947.
- [2] J. Szyszka, J. Kogut, I. Skrzypczak, and W. Kokoszka, 'Selective Internal Heat Distribution in Modified Trombe Wall', *IOP Conf. Ser. Earth Environ. Sci.*, vol. 95, p. 042018, Dec. 2017, doi: 10.1088/1755-1315/95/4/042018.
- [3] S. Sudprasert, C. Chinsorranant, and P. Rattanadecho, 'Numerical study of vertical solar chimneys with moist air in a hot and humid climate', *Int. J. Heat Mass Transf.*, vol. 102, pp. 645–656, Nov. 2016, doi: 10.1016/j.ijheatmasstransfer.2016.06.054.
- [4] H. Dahire, S. R. Kannan, and S. K. Saw, 'Effect of humidity on the performance of rooftop solar chimney', *Therm. Sci. Eng. Prog.*, vol. 27, p. 101026, Jan. 2022, doi: 10.1016/j.tsep.2021.101026.
- [5] M. A. El-Sherief, Hany. A. Mohamed, and M. Salem Ahmed, 'Design and Performance of Trombe Wall with Humidification for Air Cooling in Hot Arid Regions', *Sch. J. Eng. Technol.*, vol. 8, no. 8, pp. 147–154, Aug. 2020, doi: 10.36347/sjet. 2020.v08i08.002.
- [6] S. Zhou, F. Bai, G. Razaqpur, and B. Wang, 'Effect of key parameters on the transient thermal performance of a building envelope with Trombe wall containing phase change material', *Energy Build.*, vol. 284, p. 112879, Apr. 2023, doi: 10.1016/j.enbuild.2023.112879.
- [7] T. J. Baker, 'Fluent User's Guide', 2022.
- [8] 'JRC Photovoltaic Geographical Information System (PVGIS) European Commission'. Accessed: Jan. 11, 2024. [Online]. Available: https://re.jrc.ec.europa.eu/pvg_tools/en/
- [9] P. Liu, M. Justo Alonso, H. M. Mathisen, A. Halfvardsson, and C. Simonson, 'Understanding the role of moisture recovery in indoor humidity: An analytical study for a Norwegian single-family house during heating season', *Build. Environ.*, vol. 229, p. 109940, Feb. 2023, doi: 10.1016/j.buildenv.2022.109940.
- [10] J. Li, J. Liu, J. Pei, K. Mohanarangam, and W. Yang, 'Experimental study of human thermal plumes in a small space via large-scale TR PIV system', *Int. J. Heat Mass Transf.*, vol. 127, pp. 970–980, Dec. 2018, doi: 10.1016/j.ijheatmasstransfer.2018.07.138.
- [11] Aggarwal, 'Predicting Energy Requirement for Cooling the Building Using Artificial Neural Network', *J. Technol. Innov. Renew. Energy*, 2012, doi: 10.6000/1929-6002.2012.01.02.6.